

NANO EXPRESS

Open Access

The phase transformation of CuInS_2 from chalcopyrite to wurtzite

Bing-Bing Xie, Bin-Bin Hu, Li-Fang Jiang, Guo Li and Zu-Liang Du*

Abstract

In the present work, CuInS_2 nanoparticles have been successfully synthesized by water-bath method with deionized water as solvent and thioglycolic acid as complexing agent at 80°C . The phase transition of CuInS_2 from chalcopyrite to wurtzite was realized by adjusting the pH value of reaction solution. The emergence of Cu_2S in the condition of higher pH value of reaction solution led to the formation of wurtzite CuInS_2 . This facile method that controls the phase structure by adjusting the solution pH value could open a new way to synthesize other I-III-VI₂ ternary semiconductor compounds.

Keywords: Chalcopyrite; Wurtzite; pH; CuInS_2

Background

With increasing global energy consumption, the fabrication of pollution-free, low-cost, and high-efficiency photovoltaic cells has attracted successive attention in recent years. As an I-III-VI₂ ternary semiconductor compound with a direct bandgap of 1.5 eV at room temperature, CuInS_2 is a promising material for photovoltaic applications because of its low toxicity, high absorption coefficient, and high theoretical photovoltaic conversion efficiency (about 25% to 30%) [1-3].

In the previous studies, CuInS_2 has been found to exist in three different crystal structures: chalcopyrite, zinc blende, and wurtzite [4-6]. Chalcopyrite CuInS_2 is the most common existing phase at room temperature, whereas those with zinc blende and wurtzite structures are stable only at high temperatures. Different from those of chalcopyrite phase CuInS_2 , the indium and copper atoms of wurtzite CuInS_2 are randomly distributed over the cation sites of the lattice which allows the flexibility of stoichiometry and easily tuning the Fermi energy over a wider range [1,7,8]. Due to the differences in structure, wurtzite CuInS_2 not only exhibits different optical properties but also may present novel properties which can expand its application. Therefore, it is meaningful to develop an effective route to realize the controlled synthesis of CuInS_2 with different phase structures. Most

of the reports about controlling the phase structure of CuInS_2 were achieved by changing the ligand species or reaction temperatures. For example, Pan et al. firstly reported the synthesis of zinc blende- and wurtzite-structured CuInS_2 nanocrystals by changing the ligand species [9], and Sudip K et al. reported the synthesis of zinc blende- and wurtzite-structured CuInS_2 nanocrystals by changing the reaction temperature [10]. We also noted that for solution-phase reactions, the pH value of reaction solution can affect the complexation capability of complexing agent to metal ions, and it might be used to the control the phase structure of products. Chai et al. has reported the synthesis of cubic and hexagonal phase ZnIn_2S_4 by adjusting the pH value of the reaction solution [11]. This method presents a simple and eco-friendly way for the controlled synthesis of ternary nanomaterials with tailored structures.

On the other hand, CuInS_2 in nanophase is usually synthesized in harsh conditions of high temperature and high pressure using organic solvent, which inevitably makes the reaction more difficultly controlled. In this report, we demonstrate the successful synthesis of chalcopyrite phase and wurtzite phase CuInS_2 by a simple water-bath method at relatively low temperature of 80°C under atmospheric environment. By using deionized water as the solvent and thioglycolic acid as the complexing agent, the phase transformation of CuInS_2 from chalcopyrite phase to wurtzite phase can be achieved by

* Correspondence: zld@henu.edu.cn

Key Laboratory for Special Functional Materials of Ministry of Education, Henan University, Kaifeng 475004, Henan, People's Republic of China

simply adjusting the pH value of the reaction solution as well as the annealing temperature. It has been found that CuInS_2 gradually transformed from chalcopyrite to wurtzite with the increase of pH value, and the wurtzite CuInS_2 gradually transformed to chalcopyrite phase with the increase of annealing temperature. To the best of our knowledge, this is the first report that controls the phase transformation of CuInS_2 from chalcopyrite to wurtzite by adjusting the pH value of the reaction solution. This work may provide a feasible reference for the simple and easy synthesis of different phase-structured I-III-VI₂ ternary semiconductor compounds.

Methods

Materials

All chemicals were used as received without further purification. Copper (II) chloride dihydrate ($\text{CuCl}_2 \cdot 2\text{H}_2\text{O} \geq 99.0\%$), indium (III) sulfate anhydrous ($\text{In}_2(\text{SO}_4)_3 \geq 99.99\%$), sodium sulfide nonahydrate ($\text{Na}_2\text{S} \cdot 9\text{H}_2\text{O}$), and sodium hydroxide (2 mol/L NaOH solution) were all purchased from Tianjin Kermel Chemical Reagent Co. Ltd. (Tianjin, China). Thioglycolic acid (TGA) was obtained from Sinopharm Chemical Reagent Co. Ltd. (Shanghai, China). The water used in all experiments was obtained from a Millipore Milli-Q purification system and had a resistivity higher than $18.2 \text{ M}\Omega \cdot \text{cm}$. All experiments were carried out in water-bath pot under atmosphere.

Synthesis of CuInS_2 nanoparticles

CuInS_2 was synthesized in aqueous solution via a water-bath approach. In a typical synthesis, 1 mmol CuCl_2 and 0.5 mmol $\text{In}_2(\text{SO}_4)_3$ were mixed with 20 mL of deionized water, then TGA aqueous solution as reducing and complexing agent (20 mmol TGA in 10 mL of deionized water) was added into the solution under constant stirring. The mixture became milky white quickly. Then, the pH value of the mixed solution was adjusted from 1.27 to 10.3 by adding aqueous NaOH solution (2 mol/L) to check the effects of pH value on the final product. Na_2S aqueous solution as sulfur source (2 mmol Na_2S was dissolved in 10 mL of deionized water) was then added to the mixture. After stirring for 30 min, the reaction mixture was heated to 80°C for 48 h under atmosphere conditions. Finally, the obtained solution was cooled down to room temperature. The precipitate was separated by centrifugation and washed several times with deionized water and anhydrous ethanol then dried at 60°C for 8 h.

Characterization

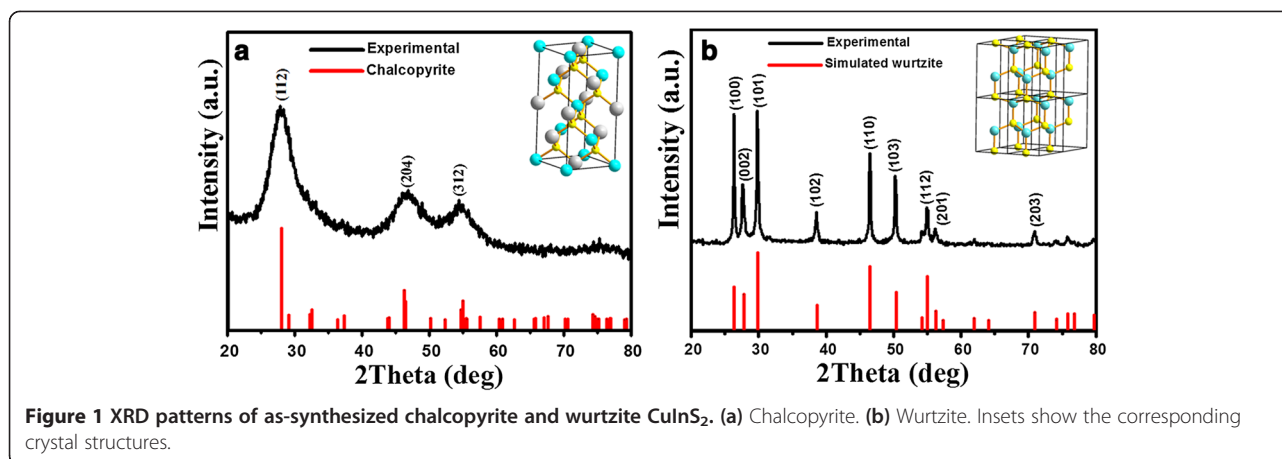
The phase and crystallographic structure of the prepared products were characterized by X-ray diffraction on a Bruker D8 Advance X-ray powder diffractometer (XRD) with Cu $K\alpha$ radiation source ($\lambda = 0.15418 \text{ nm}$). Scanning electron microscopy (SEM) images were acquired using

a FEI Nova NanoSEM 450 scanning electron microscope (FEL, Hillsboro, OR, USA). Transmission electron microscopy (TEM) images were performed on a JEOL JEM-2010 electron microscope (JEOL, Akishima-shi, Tokyo, Japan) operating at 200 kV. X-ray photoelectron spectroscopy (XPS) analysis was performed with a Kratos Axis Ultra system using monochromatic Al $K\alpha$ X-rays (1,486.6 eV). The UV-vis absorption spectra were obtained by using UV-vis Spectrometer (Perkin-Elmer, Lambda 950, Waltham, MA, USA). The simulated crystal structures and wurtzite XRD patterns of CuInS_2 were obtained by using Diamond 3.2 programs.

Results and discussion

By adjusting the pH value of the reaction solution, CuInS_2 nanoparticles with various phase structures have been successfully synthesized at the temperature of 80°C . Figure 1a shows the XRD pattern of the products synthesized with pH value of 1.27. All the diffraction peaks could be well indexed to (112), (204), and (312) planes of the standard chalcopyrite structure of CuInS_2 (JCPDS card file no. 85-1575), respectively. The diffraction peaks of the product are wide and weak, which indicates that the as-synthesized CuInS_2 nanoparticles have very small sizes or poor crystallinity [12]. Figure 1b shows the XRD pattern of the products synthesized at pH of 10.3. The peak position and relative peak intensities can match well with the powder diffraction data reported for wurtzite CuInS_2 [9,13-15]. The diffraction patterns were simulated using the lattice parameters previously reported for wurtzite CuInS_2 (simulated by using the software Diamond 3.2, with the space group of P63mc and lattice parameters $a = b = 3.897 \text{ \AA}$, $c = 6.441 \text{ \AA}$ [9]), and it matched well with our experimental XRD diffraction pattern. The diffraction peaks located at 2 theta of 26.3° , 27.69° , 29.75° , 38.52° , 46.4° , 50.32° , 54.94° , 56.3° , and 70.96° can be assigned to the (100), (002), (101), (102), (110), (103), (112), (201), and (203) planes, respectively. No diffraction peaks from other species can be detected, which indicates that the obtained samples are pure wurtzite CuInS_2 without any binary sulfides of Cu_2S , CuS , or In_2S_3 .

The morphology of the as-synthesized CuInS_2 was investigated by SEM, as shown in Figure 2. Figure 2a,d shows the SEM images of the as-synthesized chalcopyrite and wurtzite CuInS_2 , respectively. It reveals that the product is composed of a large quantity of nanoparticles, which are easily agglomerated due to the high active surface of nanoparticles. Further investigation was carried out by TEM. Figure 2b shows that the as-synthesized chalcopyrite CuInS_2 has very small sizes which match well with the obtained wide and weak XRD patterns. Figure 2e shows that the as-synthesized wurtzite CuInS_2

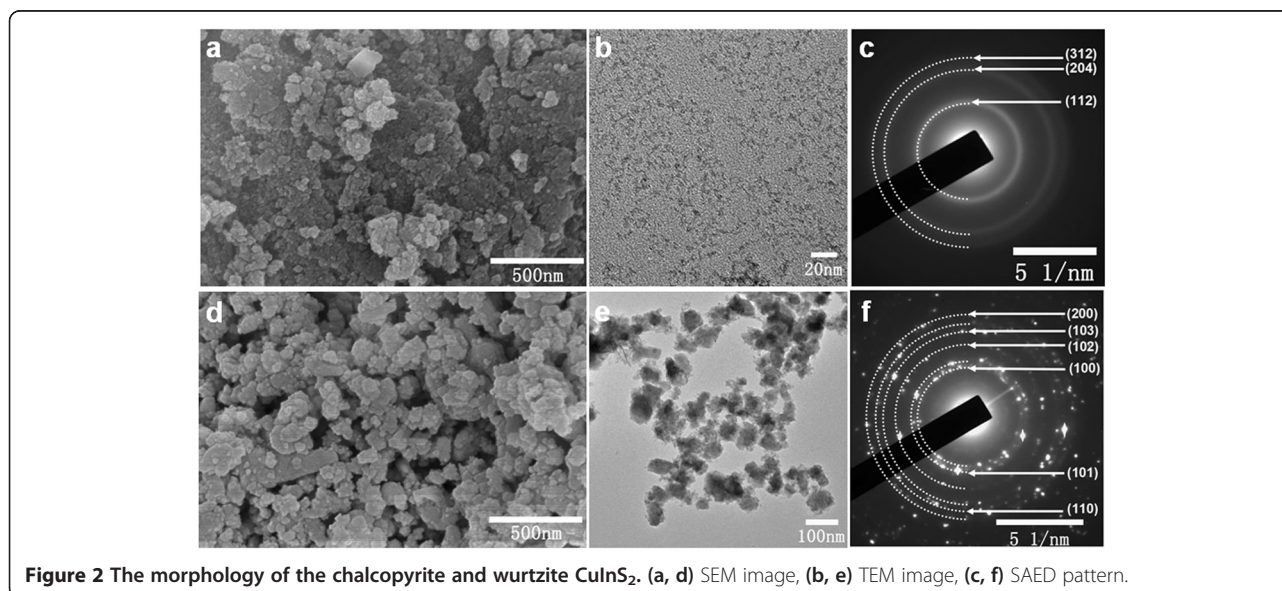


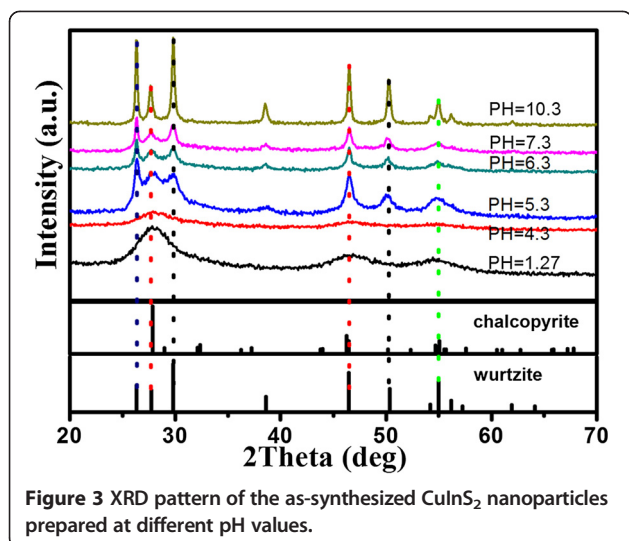
has an irregular feature of shape. Figure 2c,f shows the selected-area electron diffraction (SAED) of chalcopyrite and wurtzite CuInS_2 . In Figure 2c, three diffraction rings can be clearly seen, which can be well indexed as (112), (204), and (312) planes of the chalcopyrite CuInS_2 , respectively. Figure 2f shows the polycrystalline feature of the as-synthesized wurtzite CuInS_2 , according to the calculated lattice parameters based on the XRD pattern of wurtzite CuInS_2 . The diffraction rings can be well indexed to (100), (101), (102), (103), (110), and (200) planes of wurtzite phase CuInS_2 , respectively.

The influence of synthesis conditions on the crystal phase of products was studied by altering the pH value of reaction solution. Figure 3 shows the evolution of XRD patterns of the as-synthesized CuInS_2 nanoparticles prepared with increasing pH values of reaction solution. It was found that the pH value of reaction solution played an important role in the determination of phase

structure of the final product. As shown in Figure 3, when the pH value of the solution was 1.27, the chalcopyrite CuInS_2 could be obtained. When the pH value of the solution increased to 5.3, the chalcopyrite CuInS_2 transformed into wurtzite CuInS_2 . When the pH value of reaction solution is 10.3, the crystallization of the product is the best. Because of the Na_2S shows very strong alkaline, the final reaction solution changed to alkaline solution when sufficient Na_2S aqueous solution was added to the reaction solution with a pH value of 5.3.

According to Pearson's Hard-Soft Acid-Base (HSAB) theory [16], a soft acid and a soft base bind more tightly than a soft base and a hard acid. Cu^+ is a soft acid, In^{3+} is a hard acid, and the TGA is a soft base which will react preferentially with soft acid Cu^+ [17]. The Cu-SR bond should be stronger than the In-SR bond [12,18]. Therefore, the excess of TGA can balance the reaction rate between Cu^+ and In^{3+} and S^{2-} .





From the phenomenon of the reaction process (Additional file 1: Figure S1). When the TGA is added into the mixture solution of Cu and In ions, the color of the solution changes from blue to creamy white, which indicates that $\text{CuIn}(\text{SR})_x$ complex is generated in the solution. If the Na_2S was directly added into the solution without adjusting the pH value of the solution (pH = 1.27), the color of the solution will change from creamy white to orange. However, if the pH value of the solution was adjusted to alkalinity (pH = 10.3), the creamy white solution will become a colorless transparent solution. When we add the Na_2S into the solution, the color of solution becomes gray black.

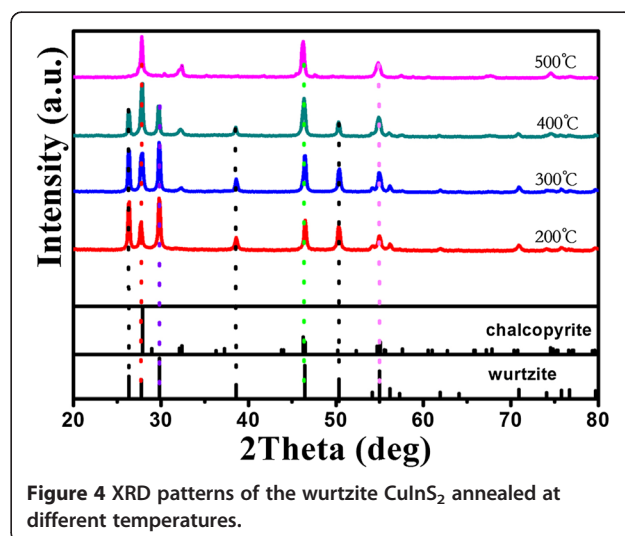
From the phenomenon of the reaction process (Additional file 1: Figure S1), It can be found that the pH value of reaction solution indeed plays an important role in the reaction. The essence is that the pH value of solution influences on the complexation of TGA. The Cu^{2+} can be quickly reduced to Cu^+ , and the $\text{CuIn}(\text{SR})_x$ complex (creamy white) is formed when the TGA is added into the mixed solution of Cu^{2+} and In^{3+} , which makes the solution change from blue to creamy white because the Cu^{2+} is blue but Cu^+ is colorless. As the pH value increases with the addition of NaOH, the $\text{CuIn}(\text{SR})_x$ complex dissociates and releases Cu^+ into solution, and the solution changes from a creamy white to a colorless transparent solution. In this case, the Cu_2S will be easily generated when Na_2S is added into the solution, which makes the mixed solution change from a colorless transparent to a gray black solution. From the XRD pattern of the as-grown products of the gray black solution (Additional file 1: Figure S2), the peaks can be well indexed to (220) and (311) planes of Cu_2S (JCPDS card file no. 02-1287), respectively, proving the formation of Cu_2S . It is the emergence of Cu_2S that leads to the formation of wurtzite CuInS_2 . Both Cu_2S and

wurtzite CuInS_2 have a hexagonal structure; such a structural similarity induces the formation of wurtzite CuInS_2 [1,19].

A series of comparative experiments have also been carried out. In any case, the pH is adjusted in the solution without TGA; the chalcopyrite nor wurtzite CuInS_2 can be synthesized. The synthesized products both in the acidic and alkaline environment are Cu (JCPDS card file no. 06-0464) and $\text{In}(\text{OH})_3$ (JCPDS card file no. 76-1464) (Additional file 1: Figure S3). It is due to the reason that the Cu^{2+} cannot be reduced to Cu^+ in the solution in the absence of TGA, and CuS is generated when the Na_2S is added. Simultaneously, Na_2S is a strong alkaline compound; as a result, $\text{In}(\text{OH})_3$ is also formed. The comparative experiment also indicates that TGA plays a crucial role for the formation of CuInS_2 because of its complexation and reducibility [20,21].

According to the previous report, metastable wurtzite CuInS_2 may transform into chalcopyrite phase when wurtzite CuInS_2 is heated to a certain temperature [6,22]. Figure 4 shows the XRD patterns of samples obtained by annealing the wurtzite phase CuInS_2 at temperatures of 200°C, 300°C, 400°C, and 500°C, respectively. It shows that the characteristic peaks at 28° of chalcopyrite become more and more obvious with the increase of annealing temperatures. When the metastable wurtzite CuInS_2 was annealed from 200°C to 400°C, a coexistence stage of chalcopyrite phase and wurtzite phase CuInS_2 might exist. When the temperature reached 500°C, the wurtzite phase CuInS_2 completely transformed into chalcopyrite phase.

The chemical composition and valence states of wurtzite CuInS_2 were investigated by XPS analysis. The typical survey and high-resolution spectra in regions of Cu 2p, In 3d, and S 2p are shown in Figure 5. The survey spectrum in Figure 5a indicates that the product



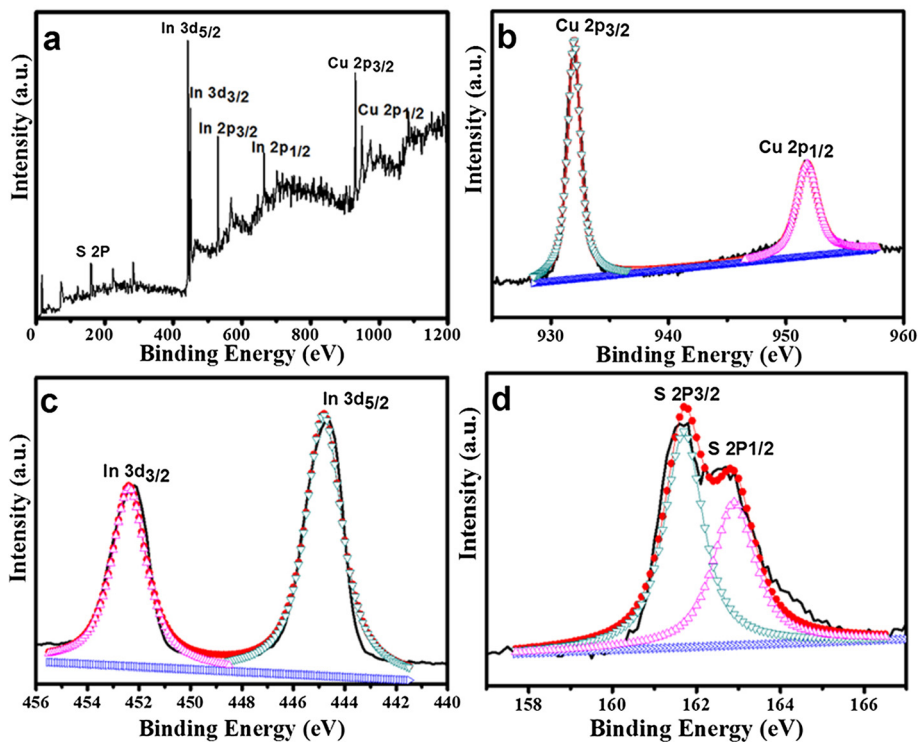


Figure 5 The XPS spectra of wurtzite CuInS_2 . (a) Survey spectrum, (b) Cu 2p, (c) In 3d, (d) S 2p.

contains Cu, In, and S elements. As shown in Figure 5b, the binding energies of Cu $2p_{3/2}$ and $2p_{1/2}$ were located at 931.9 and 951.7 eV with a peak splitting of 19.8 eV, respectively, which are in good consistency with the reported values for Cu^+ [10,23]. In addition, the Cu $2p_{3/2}$

satellite peak of Cu^{2+} , which is usually located at 942 eV, does not appear in the spectra [24]. Therefore, it can be concluded that the starting Cu^{2+} ions have been reduced to Cu^+ by TGA. The In $3d_{5/2}$ and $3d_{3/2}$ peaks (Figure 5c) were located at 444.7 and 452.3 eV with a peak splitting

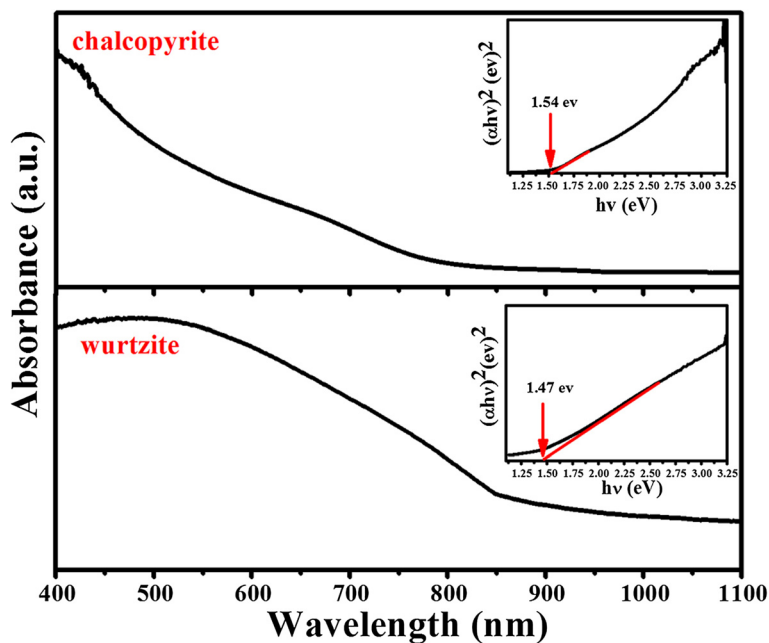


Figure 6 The UV-vis absorption spectrum of chalcopyrite and wurtzite CuInS_2 . The insets show the bandgaps of the CuInS_2 .

of 7.6 eV, which matched well with that of In^{3+} . The S 2p has doublet peaks of S 2p_{1/2} and 2p_{3/2} due to the spin-orbit coupling [25]. The two peaks of S 2p (Figure 5d) were located at 161.7 and 162.8 eV, respectively, with a peak splitting of 1.1 eV, which can be assigned to S^{2+} . No obvious impurities could be detected in the sample.

Figure 6 shows the UV-vis absorption spectrum of the as-prepared chalcopyrite and wurtzite CuInS_2 measured at room temperature. Both the two phases of CuInS_2 show a broad and strong absorption in the visible region. Compared with chalcopyrite CuInS_2 , the wurtzite CuInS_2 showed a higher and broader absorption in the entire visible region and near-infrared region. The bandgap can be determined by plotting $(\alpha h\nu)^2$ versus $h\nu$ (α = absorbance, h = Planck's constant, and ν = frequency) [26,27]. As shown in the inset picture, the calculated optical bandgap for chalcopyrite and wurtzite CuInS_2 is about 1.54 and 1.47 eV, respectively, which is close to the bulk energy bandgap of CuInS_2 .

Conclusions

In summary, CuInS_2 in chalcopyrite and wurtzite phases has been successfully synthesized via a low-cost, facile water-bath method. The phase structure of as-synthesized CuInS_2 can be easily controlled by adjusting the pH value of the reaction solution. Low-cost thioglycolic acid plays a key role in the synthesis process of CuInS_2 . Thioglycolic acid acts not only as a stabilizer and complexing agent to balance the reaction rate among Cu^+ , In^{3+} , and S^{2-} but also as a reducing agent which can reduce Cu^{2+} to Cu^+ . Compared with the traditional organic phase synthesis route, this method provides a feasible way that is much simpler, greener, and cheaper, in addition to the easy control of phase structure for the mass production of CuInS_2 .

Additional file

Additional file 1: Figure S1. The phenomenon of the reaction process.
Figure S2. XRD pattern of the as-grown products of gray black solution.
Figure S3. XRD pattern of the products synthesized without thioglycolic acid.

Competing interests

The authors declare that they have no competing interests.

Authors' contributions

BBX and BBH carried out the experiments and wrote the manuscript. LFJ and GL participated in the experiment design and characterization of the sample. ZLD was the investigator who guided the whole experiments and the draft of the manuscript. All authors read and approved the final manuscript.

Acknowledgment

This work was supported by the National Natural Science Foundation of China (nos. 20371015, 10874040, 20903034, and 21203055), the Cultivation Fund of Key Scientific and Technical Innovation Project, Ministry of Education of China (no. 708062), Basic and Frontier Research Program of Science and Technology Department of Henan Province (no. 112300410277), and the

Program for Changjiang Scholars and Innovative Research Team in University (no. PCS IRT1126). BBH and BBX contributed equally to this paper.

Received: 20 December 2014 Accepted: 4 February 2015

Published online: 27 February 2015

References

- Connor ST, Hsu CM, Weil BD, Aloni S, Cui Y. Phase transformation of biphasic $\text{Cu}_2\text{S-CuInS}_2$ to monophasic CuInS_2 nanorods. *J Am Chem Soc.* 2009;131:4962–6.
- Yu YX, Ouyang WX, Liao ZT, Du BB, Zhang WD. Construction of $\text{ZnO/ZnS/CdS/CuInS}_2$ core-shell nanowire arrays via ion exchange: p-n junction photoanode with enhanced photoelectrochemical activity under visible light. *ACS Appl Mater Interfaces.* 2014;6:8467–74.
- Norako ME, Franzman MA, Brutchey RL. Growth kinetics of monodisperse Cu-In-S nanocrystals using a dialkyl disulfide sulfur source. *Chem Mater.* 2009;21:4299–304.
- Binsma JJM, Gilling LJ, Bloem J. Phase relations in the system $\text{Cu}_2\text{S-In}_2\text{S}_3$. *J Cryst Growth.* 1980;50:429.
- Lu XT, Zhuang ZB, Peng Q, Li YD. Controlled synthesis of wurtzite CuInS_2 nanocrystals and their side-by-side nanorod assemblies. *CrystEngComm.* 2011;13:4039–45.
- Gusain M, Kumar P, Nagarajan R. Wurtzite CuInS_2 : solution based one pot direct synthesis and its doping studies with non-magnetic Ga^{3+} and magnetic Fe^{3+} ions. *RSC Advances.* 2013;3:18863–71.
- Qi YX, Liu QC, Tang KB, Liang ZH, Ren ZB, Liu XM. Synthesis and characterization of nanostructured wurtzite CuInS_2 : a new cation disordered polymorph of CuInS_2 . *J Phys Chem C.* 2009;113:3939–44.
- Kruszynska M, Borchert H, Parisi J, Kolny-Olesiak J. Synthesis and shape control of CuInS_2 nanoparticles. *J Am Chem Soc.* 2010;132:15976–86.
- Pan DC, An LJ, Sun ZM, Hou WL, Yang Y, Yang ZZ, et al. Synthesis of Cu-In-S ternary nanocrystals with tunable structure and composition. *J Am Chem Soc.* 2008;130:5620–1.
- Sudip KB, Tian L, Venkatram N, Wei J, Vittal JJ. Phase-selective synthesis of CuInS_2 nanocrystals. *J Phys Chem C.* 2009;113:15037–42.
- Chai B, Peng TY, Zeng P, Zhang XH, Liu XJ. Template-free hydrothermal synthesis of ZnIn_2S_4 flower-like microspheres as an efficient photocatalyst for H_2 production under visible-light irradiation. *J Phys Chem C.* 2011;115:6149–55.
- Zhong HZ, Lo SS, Mirkovic T, Li YC, Ding YQ, Li YF, et al. Noninjection gram-scale synthesis of monodisperse pyramidal CuInS_2 nanocrystals and their size-dependent properties. *ACS NANO.* 2012;9:5253–62.
- Wang Y, Zhao XD, Liu FY, Zhang XH, Chen HW, Bao FX, et al. Selective synthesis of cubic and hexagonal phase of CuInS_2 nanocrystals by microwave irradiation. *RSC Advance.* 2014;4:16022–6.
- Yu C, Zhang LL, Tian L, Liu D, Chen FL, Wang C. Synthesis and formation mechanism of CuInS_2 nanocrystals with a tunable phase. *CrystEngComm.* 2014;16:9596–602.
- Sheng X, Wang L, Luo YP, Yang DR. Synthesis of hexagonal structured wurtzite and chalcopyrite CuInS_2 via a simple solution route. *Nanoscale Res Lett.* 2011;6:562.
- Pearson RG. Hard and soft acids and bases. *J Am Chem Soc.* 1963;85:3533–9.
- Regulacio MD, Win KY, Lo SL, Zhang SY, Zhang XH, Wang S, et al. Aqueous synthesis of highly luminescent $\text{AgInS}_2\text{-ZnS}$ quantum dots and their biological applications. *Nanoscale.* 2013;5:2322–7.
- Yu K, Peter NG, Ouyang JY, Zaman MB, Abulrob A, Baral TN, et al. Low-temperature approach to highly emissive copper indium sulfide colloidal nanocrystals and their bioimaging applications. *ACS Appl Mater Interfaces.* 2013;5:2870–80.
- Li J, Bloemen M, Parisi J, Kolny-Olesiak J. Role of copper sulfide seeds in the growth process of CuInS_2 nanorods and networks. *ACS Appl Mater Interfaces.* 2014;6:20535–43.
- Gou XL, Peng SG, Zhang L, Shi YH, Chen J, Shen PW. Thioglycolic acid-assisted solvothermal synthesis of CuInS_2 with controllable microstructures. *Chem Lett.* 2006;9:1050–1.
- Chen YY, Li SJ, Huang LJ, Pan DC. Low-cost and gram-scale synthesis of water-soluble Cu-In-S/ZnS core/shell quantum dots in an electric pressure cooker. *Nanoscale.* 2014;6:1295–8.
- Zhou WH, Jiao J, Zhao Y, Cheng XY, Kou DX, Zhou ZJ, et al. Synthesis of metastable wurtzite CuInS_2 nanocrystals and films from aqueous solution. *RSC Advance.* 2014;4:7617–22.

23. Wang JJ, Wang YQ, Cao FF, Guo YG, Wan LJ. Synthesis of monodispersed wurtzite structure CuInSe_2 nanocrystals and their application in high-performance organic-inorganic hybrid photodetectors. *J Am Chem Soc.* 2010;132:12218–21.
24. Lei SJ, Wang CY, Liu L, Guo DH, Wang CN, Tang QL, et al. Spinel indium sulfide precursor for the phase-selective synthesis of Cu-In-S nanocrystals with zinc-blende, wurtzite, and spinel structures. *Chem Mater.* 2013;25(15):2991–7.
25. Zhong HZ, Zhou Y, Ye MF, He YJ, Ye JP, He C, et al. Controlled synthesis and optical properties of colloidal ternary chalcogenide CuInS_2 nanocrystals. *Chem Mater.* 2008;20:6434–43.
26. Chang J, Waclawik ER. Controlled synthesis of CuInS_2 , Cu_2SnS_3 , and $\text{Cu}_2\text{ZnSnS}_4$ nanostructures: insight into the universal phase-selectivity mechanism. *CrystEngComm.* 2013;15:5612–9.
27. Wang YH, Zhang XY, Bao NZ, Lin BP, Gupta A. Synthesis of shape controlled monodisperse wurtzite $\text{CuIn}_x\text{Ga}_{1-x}\text{S}_2\text{Se}$ semiconductor nanocrystals with tunable band gap. *J Am Chem Soc.* 2011;133:11072–5.

Submit your manuscript to a SpringerOpen[®] journal and benefit from:

- Convenient online submission
- Rigorous peer review
- Immediate publication on acceptance
- Open access: articles freely available online
- High visibility within the field
- Retaining the copyright to your article

Submit your next manuscript at ► springeropen.com
